Molecular Biology of the Cell
Vol. 19, 553–562, February 2008

Myosin Transducer Mutations Differentially Affect Motor Function, Myofibril Structure, and the Performance of Skeletal and Cardiac Muscles

Anthony Cammarato,*† Corey M. Dambacher,*‡ Aileen F. Knowles,§ William A. Kronert,* Rolf Bodmer,† Karen Ocorr,† and Sanford I. Bernstein*

*Department of Biology and Heart Institute, San Diego State University, San Diego, CA 92182-4614; †Development and Aging Program, Burnham Institute for Medical Research, La Jolla, CA 92037; and §Department of Chemistry and Biochemistry, San Diego State University, San Diego, CA 92182-1030

Submitted September 12, 2007; Revised November 6, 2007; Accepted November 16, 2007
Monitoring Editor: Thomas Pollard

Striated muscle myosin is a multidomain ATP-dependent molecular motor. Alterations to various domains affect the chemomechanical properties of the motor, and they are associated with skeletal and cardiac myopathies. The myosin transducer domain is located near the nucleotide-binding site. Here, we helped define the role of the transducer by using an integrative approach to study how *Drosophila melanogaster* transducer mutations *D45* and Mhc^5 affect myosin function and skeletal and cardiac muscle structure and performance. We found *D45* (A261T) myosin has depressed ATPase activity and in vitro actin motility, whereas Mhc^5 (G200D) myosin has these properties enhanced. Depressed *D45* myosin activity protects against age-associated dysfunction in metabolically demanding skeletal muscles. In contrast, enhanced Mhc^5 myosin function allows normal skeletal myofibril assembly, but it induces degradation of the myofibrillar apparatus, probably as a result of contractile disinhibition. Analysis of beating hearts demonstrates depressed motor function evokes a dilatory response, similar to that seen with vertebrate dilated cardiomyopathy myosin mutations, and it disrupts contractile rhythmicity. Enhanced myosin performance generates a phenotype apparently analogous to that of human restrictive cardiomyopathy, possibly indicating myosin-based origins for the disease. The *D45* and Mhc^5 mutations illustrate the transducer's role in influencing the chemomechanical properties of myosin and produce unique pathologies in distinct muscles. Our data suggest *Drosophila* is a valuable system for identifying and modeling mutations analogous to those associated with specific human muscle disorders.

INTRODUCTION

The myosin molecular motor of striated muscle is a hexameric molecule composed of two myosin heavy chains (MHCs) and four light chains. The N-terminal globular motor domain is a product inhibited ATPase comprised of several communicating domains and functional units (reviewed by Geeves and Holmes, 1999, 2005; Geeves *et al*., 2005). Alterations to the various domains dramatically affect the biochemical and mechanical properties of the motor in vitro, and mutations that diminish or enhance the molecular performance of myosin in vivo are associated with the pathogenesis of both skeletal and cardiac myopathies (reviewed by Sellers, 1999; Redowicz, 2002; Oldfors *et al*., 2004; Chang and Potter, 2005; Laing and Nowak, 2005; Tardiff, 2005; Oldfors, 2007). Central to an understanding of myosin-based myopathies is a fundamental appreciation for how depressed or enhanced molecular motor function differentially affects diverse striated muscles.

Among the communicating functional units of myosin is the recently described transducer region (Coureux *et al*., 2004). Myosin V crystal structures reveal the transducer's central location within the motor domain near the nucleotide binding site. The transducer includes the last three strands of a seven-stranded β-sheet, which undergoes distortion essential for rearrangements within the nucleotide pocket during the ATPase cycle, and the loops and linkers that accommodate the distortion (Coureux *et al*., 2004). Among the elements of the transducer is hypervariable loop 1, a flexible surface loop shown to influence a wide range of kinetic and mechanical properties of myosin (Kurzawa-Goertz *et al*., 1998; Sweeney *et al*., 1998; Clark *et al*., 2005). The transducer ultimately integrates information from all parts of the motor domain to facilitate efficient conversion of the energy liberated during ATP hydrolysis into force production (Coureux *et al*., 2004).

In striated muscle, myosin-containing thick filaments drive contraction in an ATP-dependent manner through cyclical interactions with actin-containing thin filaments. The thin filament troponin–tropomyosin regulatory complex inhibits contraction in resting muscle by occluding

This article was published online ahead of print in *MBC in Press* (http://www.molbiolcell.org/cgi/doi/10.1091/mbc.E07–09–0890) on November 28, 2007.

‡ Present address: The Scripps Research Institute, Kellogg School of Science and Technology, 10550 N. Torrey Pines Rd., TPC-19, La Jolla, CA 92037.

Address correspondence to: Sanford I. Bernstein (sbernst@sciences.sdsu.edu) or Karen Ocorr (kocorr@burnham.org).

Abbreviations used: AI, arrythmicity index; DCM, dilated cardiomyopathy; DI, diastolic interval; FI, flight index; HP, heart period; IFI, indirect flight isoform; IFM, indirect flight muscle; MHC, myosin heavy chain; RCM, restrictive cardiomyopathy; SI, systolic interval; Tn, troponin.

myosin binding sites on actin (reviewed by Gordon *et al.*, 2000; Brown and Cohen, 2005). On activation, tropomyosin shifts positions in a stepwise manner away from these binding sites, first as a result of Ca^{2+} binding to troponin and then by myosin cross-bridge binding to actin (McKillop and Geeves, 1993; Vibert *et al.*, 1997; Poole *et al.*, 2006). Initial cross-bridge binding to actin seems to have allosteric effects on thin filaments such that there is a spread of accessible myosin binding sites along the filaments leading to cooperative activation of contraction (reviewed by Tobacman, 1996; Gordon *et al.*, 2000; Moss *et al.*, 2004). Thus, both elevated Ca^{2+} levels and cross-bridge binding are required for full activation.

Investigations of the functional domains of myosin and the effects of mutations on muscle contractile properties are greatly facilitated by studying the genetically tractable *Drosophila melanogaster* system. The *Drosophila Mhc* gene exists as a single copy per haploid genome that encodes all muscle MHCs through alternative splicing of the primary transcript (Bernstein *et al.*, 1983; Rozek and Davidson, 1983; George *et al.*, 1989). Nonlethal mutations located in constitutive exons are expressed in all myosin isoforms of every striated muscle. Consequently, in such mutants, unlike in vertebrate systems possessing complex *Mhc* multigene families, compensatory up-regulation of nonmutated myosin isoforms cannot occur. Furthermore, changes in striated muscle performance due to developmental or senescent-dependent switches in myosin isoform complements lacking the mutations are impossible.

The effects of particular myosin isoforms on muscle function during aging can be readily studied in *Drosophila*. Muscles amenable to such analyses include indirect fight (IFM) (Baker, 1976; Magwere *et al.*, 2006) and cardiac muscles (Paternostro *et al.*, 2001; Wolf *et al.*, 2006; Ocorr *et al.*, 2007). IFM function is not required for viability, and *Drosophila* cardiac function can be dramatically compromised without causing immediate death. *Drosophila* age in weeks, and they share common mechanisms that determine aging rates and longevity with higher organisms (Parkes *et al.*, 1999; Finch and Ruvkun, 2001; Tatar *et al.*, 2003; Wessells and Bodmer, 2007). Thus, the fly is an extremely powerful model for studying the progression of myosin-related skeletal and cardiac muscle dysfunction.

Two myosin point mutations in the *Drosophila Mhc* gene, *D45* and *Mhc*^{5}, were localized in proximity to coding regions for loops and linkers of the transducer (Kronert *et al.*, 1999; Montana and Littleton, 2004). These mutations are in *Mhc* constitutive exons 5 and 4, respectively. Both mutations impair *Drosophila* flight ability, and they either suppress (*D45*) or enhance (*Mhc*^{5}) IFM myofibrillar destruction when combined with certain troponin mutations (Kronert *et al.*, 1999). These findings suggest the amino acid changes differentially alter the fundamental chemomechanical properties of myosin and possibly mimic perturbations in motor function caused by certain myosin-based myopathy mutations. Because every isoform of striated muscle myosin from the two lines possesses the alterations, the mutants are unique tools for examining the pathophysiological responses to perturbed motor function in distinct striated muscles of a single model organism.

Here, we provide the first detailed analysis of the effects of mutations in specific transducer elements on myosin molecular function and on age-related changes in skeletal and cardiac muscles. To identify changes in molecular motor performance, myosin was purified from IFM of wild-type and mutant flies for biochemical and biophysical analyses. Skeletal muscle locomotory function was assessed by evaluating flight abilities of wild-type and transducer mutant flies throughout life. We used electron microscopy to evaluate the consequences of mutant myosin expression on IFM myofibrillar ultrastructure. We additionally investigated the progressive changes in cardiac structure and function as a result of altered motor properties by using high-speed video microscopy and advanced motion detection analysis. Our efforts to define the role of the transducer in determining chemomechanical properties of myosin and in diverse striated muscles demonstrate that *Drosophila* is useful for investigating the pathogenesis of skeletal and cardiac disorders. Furthermore, our model may serve to identify novel mutations that lead to specific myopathies found in the human population.

MATERIALS AND METHODS

Fly Lines and Aging

yw (wild-type), *D45*, and *Mhc*^{5} *Drosophila* were maintained on a standard yeast-sucrose-agar medium at 25°C. For flight and cardiac muscle studies, newly eclosed flies were collected over an 8-h span. All flies were transferred to fresh vials every 2–3 d over a 5-wk period.

Protein Isolation and Purification

IFM myosin was purified from 1- to 2-d-old *yw* or mutant flies as described previously (Swank *et al.*, 2001) with the following modifications: 10 mM dithiothreitol (DTT) in distilled H_2O was used for all dilutions, and all solution volumes were decreased to 75% of previously published volumes. Purified myosin pellets were resuspended in myosin storage buffer consisting of 0.5 M KCl, 20 mM 3-(*N*-morpholino)propanesulfonic acid, pH 7.0, 2 mM $MgCl_2$, and 20 mM DTT. Subsequent biochemical and mechanical experiments were performed immediately after spectroscopic methods (Margossian and Lowey, 1982) for determining myosin concentrations.

ATPase Assays

Myosin ATPase activities were determined using [γ-^{32}P]ATP. Ca^{2+} ATPase was measured as described previously (Swank *et al.*, 2001). Actin-activated ATPase was determined using chicken skeletal muscle actin (Swank *et al.*, 2003). G-actin was isolated from acetone powder of chicken skeletal muscle according to Pardee and Spudich (1982). F-actin was prepared by adding 1 volume of 10X polymerization buffer (50 mM Tris-Cl, pH 8, 0.5 M KCl, 20 mM $MgCl_2$, and 10 mM ATP) to 9 volumes of G-actin. The working F-actin solution had a concentration of ~30 μM, so that the amount of nonradioactive ATP added to the reaction mixture was minimized. Actin-activated V_{max} and K_m values for actin were computed by fitting all data points from multiple preparations of each myosin isoform (wild type [n = 9], *D45* [n = 4], or *Mhc*^{5} [n = 3]) with the Michaelis-Menten equation. Values were averaged to give mean ± SD. Statistical differences in V_{max} and K_m between wild-type and mutant myosin isoforms were evaluated using Student's *t* tests.

In Vitro Motility Assays

In vitro actin sliding velocity was determined according to Swank *et al.* (2001), with some alterations: 20 mM DTT was used in all solutions of the assay. The 0 salt motility assay buffer/0.4% methyl cellulose/glucose oxidase and catylase (0B/MC/GOC) and 0B/MC/GOC + ATP (0B/MC/GOC with 2 mM ATP added) solutions were diluted to 70% of that used previously. Lower ionic strength elevated levels of continuous movement for the majority of actin filaments. Analysis of captured video sequences was performed as described by Root and Wang (1994), by using the modifications described in Swank *et al.* (2001). Velocities of 15–20 individual filaments were calculated and recorded from each assay; values from multiple preparations (wild-type [n = 4], *D45* [n = 4], or *Mhc*^{5} [n = 3]) were averaged to give mean ± SD. Statistical differences in the average velocity of actin filaments driven by wild-type and mutant myosin isoforms were determined by Student's *t* tests.

Flight Testing

Flight testing of 2-, 7-, 21-, or 35-d-old flies was performed as described in Drummond *et al.* (1991) and Suggs *et al.* (2007). Each fly was assigned a flight index (FI) value based on its ability to fly up (6), horizontal (4), downward (2), or not at all (0). The average FI (±SD) for each line was calculated by dividing the sum of the individual FI values by the number of individuals tested ($n > 200$) at each age point. Statistical testing of age-associated changes in mean FI among groups and within each line was performed as described below for calculating differences in age-dependent changes in cardiac parameters between and within genotypes.

Electron Microscopy of Drosophila IFM

Thoraces from late pupa and 2-d-old female flies were isolated and prepared for transmission electron microscopy according to Cripps *et al.* (1994). Fixatives and Embed812 resin were purchased from Electron Microscopy Sciences (Fort Washington, PA); other reagents were purchased from Sigma-Aldrich (St. Louis, MO). Late pupal and 2-d-old adult samples were examined on a Philips 410 transmission electron microscope operating at 80 kV. Images were recorded on film and later digitized using an Epson 1640SU PHOTO flatbed scanner. Young adult and some pupal samples were examined with a FEI Tecnai 12 transmission electron microscope operating at 120 kV. Digital images were taken with a TemCam-F214 high-resolution digital camera (TVIPS-Tietz, Gauting, Germany). Microscope magnifications were calibrated using a diffraction grating replica and latex calibration standard (Ted Pella, Redding, CA).

Image Analysis of Semi-intact Heart Preparations

Image analysis of beating, semi-intact heart preparations from 1-, 2-, 3-, 4-, and 5-wk-old adults was performed according to Ocorr *et al.* (2007). M-modes were generated using a MatLab (MathWorks, Natick, MA)-based image analysis program (Ocorr *et al.*, 2007). Briefly, a 1 pixel-wide region is defined in a single frame of a high-speed digital movie that encompasses both edges of the heart tube; identical regions are then cut from all consecutive movie frames and aligned horizontally. This provides an edge trace that documents the movement of the heart tube walls in the *y*-axis over time in the *x*-axis.

Measurements of diastolic and systolic diameters were made within the third abdominal segment of heart tubes directly from individual video frames. These and other cardiac contractile parameters were obtained as output from the MatLab-based program. Heart periods (HP) are defined as the time between the ends of two consecutive diastolic intervals. The arrythmicity index (AI) was calculated as the standard deviations of all recorded HP for an individual fly normalized to the median HP for that fly. Large standard deviations in HP for a single fly are a reflection of nonuniformly rhythmic contraction/relaxation cycles.

Age-dependent changes in cardiac parameters were modeled hierarchically. For all analyses, values of $p < 0.05$ were considered significant. Measured parameters included cardiac diameters (diastolic and systolic wall distances), percentage of fractional shortening, HP, diastolic intervals (DIs) and systolic intervals (SIs), and AI. For each fly line, we initially fit a linear model to the mean parameter values from 1 through 5 wk of age. We estimated potential nonlinear change through time using an added sums of squares F-test. For all cardiac parameters, except diastolic distances, there was no strong evidence ($p > 0.05$) of significant nonlinear change through time. Although diastolic heart wall distance changes with age did reveal statistical evidence of nonlinearity ($p = 0.03$), the deviation was considered minor; therefore, these and all other response variables were fit with linear models. Analysis of covariance (ANCOVA) was used to test for heterogeneities in the slopes of the fitted lines from each genotype, for each parameter. When significant heterogeneity in slopes was found, we estimated the different functional relationships (slopes) by regression analysis, and we tested for significant change with respect to age. If no significant heterogeneity was found among the slopes, a common slope was estimated via linear regression. We determined whether the common slope, shared among groups, was significant and we performed multiple comparisons among the elevations of the lines to investigate statistical differences between the genotypes. Analysis of variance (ANOVA) for genotype as a function of SI was used to test whether significant differences between *yw* and *Mhc*^{5} existed at each of the five age points.

RESULTS

D45 and Mhc^5 *Mutations Reside within Distinct Transducer Elements*

The *D. melanogaster Mhc* mutants *D45* and *Mhc*^{5} contain single amino acid conversions previously localized to the vicinity of ATP entry and the ATP binding site on chicken skeletal myosin S1 fragment (Kronert *et al.*, 1999). It was postulated that both mutations affect the ATPase cycle by regulating nucleotide entry or product release from the binding pocket (Kronert *et al.*, 1999). Mapping the point mutations onto chicken myosin V motor domain structures reveals that the specific amino acid alterations reside within distinct structural elements of the transducer region (Figure 1A) (Coureux *et al.*, 2003, 2004). The *D45* (A261T) mutation occurs at the junction between the β-bulge and the seventh strand of the central β-sheet, whereas the *Mhc*^{5} mutation (G200D) maps close to the junction between the HF helix and loop 1. Sequence comparisons corroborate the locations of the *Drosophila* mutations relative to specific transducer elements from different organisms (Figure 1B). The alignments also demonstrate the variability found within loop 1 primary structures among various myosin isoforms. The structural elements of the transducer were proposed to interact in a coordinated manner to bring about kinetic tuning of product release after ATP hydrolysis (Coureux *et al.*, 2004). Point mutations within the transducer may alter rates of transitions between states of the actomyosin ATPase cycle and thereby influence chemomechanical transduction in the muscles in which they are expressed.

Biochemical and Mechanical Properties of the Mutant Myosin Isoforms

To determine the effects of distinct transducer mutations on the biochemical and molecular mechanical properties of my-

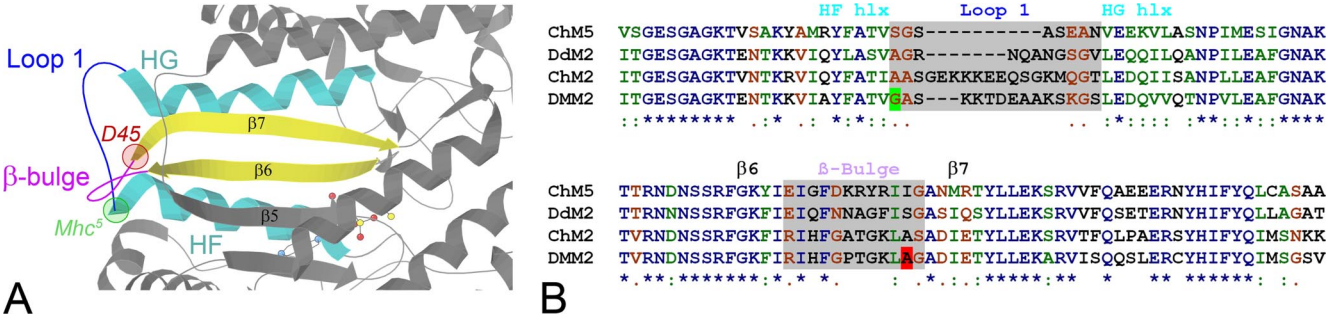

Figure 1. Locations of myosin transducer mutations and the alignment and sequence comparison of transducer elements from various myosin isoforms. (A) Ribbon diagram (prepared using the KiNG 1.39 [Kinemage, Next Generation, Durham, NC] interactive system for three-dimensional vector graphics) of a portion of the chicken myosin V (Protein Data Bank code 1W7J) motor domain near the nucleotide (shown as a ball and stick model) binding pocket, with specific components of the transducer region labeled. The locations of *D. melanogaster D45* and *Mhc*^{5} mutations are shown relative to specific transducer elements. *D45* is at the junction between the β-bulge and the seventh strand of the central β-sheet, whereas *Mhc*^{5} lies close to the junction between the HF helix and hypervariable loop 1. (B) ClustalW amino acid alignment of specific MHC regions from ChM5, *Gallus gallus* (chicken) myosin Va; DdM2, *Dictyostelium discoideum* nonmuscle myosin II; ChM2, *G. gallus* skeletal muscle myosin II; and DMM2, *D. melanogaster* muscle myosin II. (*), fully conserved residues; (:), conservation of strong groups; and (.), conservation of weak groups. DMM2 sequences reveal the locations of the *Mhc*^{5} (G200D) mutation (green) and the *D45* (A261T) mutation (red) relative to specific transducer elements (chicken numbering system). The sequences and designations of the HF helix (hlx), Loop 1, HG hlx, β-strand 6 (β6), β-bulge, and β7 are based on the sequences of key structural elements of chicken myosin V and *Dictyostelium* myosin II motors as described in Coureux *et al.* (2004) Supplementary Table 8.

Table 1. Wild-type (IFI) and mutant myosin biochemical and mechanical data

	Ca^{2+} ATPase (s^{-1})	Mg^{2+} ATPase (s^{-1})	V_{max} (s^{-1}) Actin-ATPase	K_m, Actin (μM) Actin-ATPase	In vitro motility (μm/s)
IFI	6.95 ± 1.43 (9)	0.203 ± 0.063	1.83 ± 0.061	0.28 ± 0.050	7.44 ± 0.73 (4)
D45	5.42 ± 1.13 (4)	0.106 ± 0.037*	0.69 ± 0.077*	0.30 ± 0.014	3.47 ± 0.57* (4)
Mhc^5	5.16 ± 1.17 (3)	0.482 ± 0.097*	1.47 ± 0.084*	0.23 ± 0.014	8.69 ± 0.50* (3)

Values in parentheses denote the number of myosin preparations used to generate mean values for ATPase and in vitro motility assays. SD values are provided for all measured parameters.

* Values are statistically different ($p < 0.001$) from those obtained for the IFI.

osin in vitro, we measured Ca^{2+}, Mg^{2+}, and actin-stimulated ATPase activities, determined K_m values for actin, and performed in vitro motility assays on the wild-type indirect flight isoform (IFI) and mutant IFM myosin (see Table 1). Basal Ca^{2+} ATPase activities of purified *D45* and *Mhc*^{5} myosin were similar to the IFI. However, basal Mg^{2+} ATPase activity for *D45* myosin was about half that of the IFI, whereas basal Mg^{2+} ATPase activity for *Mhc*^{5} myosin was more than twofold higher than for the IFI. Maximum actin-activated ATPase activity (V_{max}) (Figure 2A) for *D45* myosin was almost threefold lower than that of the IFI, and it was approximately twofold lower than that of *Mhc*^{5} myosin. K_m, a measure of actin-binding affinity, for either transducer mutant did not differ significantly from that for wild-type myosin. In vitro motility assays (Table 1 and Figure 2B), performed using *D45* myosin displayed a reduction in actin filament translocation to about half the velocity of the IFI. Myosin containing the *Mhc*^{5} mutation increased actin velocity roughly 15%. Thus, distinct mutations in the transducer region elicit opposing effects on myosin. The *D45* mutation depresses the biochemical and mechanical functions of the motor, whereas the *Mhc*^{5} mutation enhances them.

Effects of Mutant Myosin on Skeletal Muscle Function

Because the *D. melanogaster* transducer is conserved in every striated muscle myosin isoform, we investigated the effects of depressed or enhanced molecular motor function on distinct muscles with differing physiological roles and properties. We assessed skeletal muscle function by evaluating age-dependent changes in flight ability. Wild-type (*yw*) flies expressing IFI myosin showed a characteristically rapid and steady decline in flight ability from 2 d through 5 wk of age (Figure 2C). Over 35 d, there was an ~60% overall decrease in FI. In addition to exhibiting an ~20% reduction in initial flight ability, relative to *yw*, *D45* flies also showed a significant decrease in FI over the 35-d period. However, the rate of decline was less and the overall decrease was only ~30%, which was markedly lower than wild type. Thus, hypoactive flight muscle myosin expressed in *D45* flies provided protection against normal age-dependent muscle dysfunction. Conversely, flies expressing hyperactive *Mhc*^{5} myosin showed no flight ability at any age.

Effects of Mutant Myosin on Skeletal Muscle Ultrastructure

To ascertain whether expression of myosin with depressed or enhanced ATP hydrolytic and mechanical properties produced ultrastructural abnormalities within skeletal muscles, we examined the IFM by transmission electron microscopy (Figure 3, A–D). Longitudinal and transverse sections revealed that *D45* myosin expression (Figure 3B) did not disrupt the assembly or integrity of myofibrils within the IFM, because their general appearance closely resembled that of *yw* myofibrils (Figure 3A). Sarcomeric structure in both lines

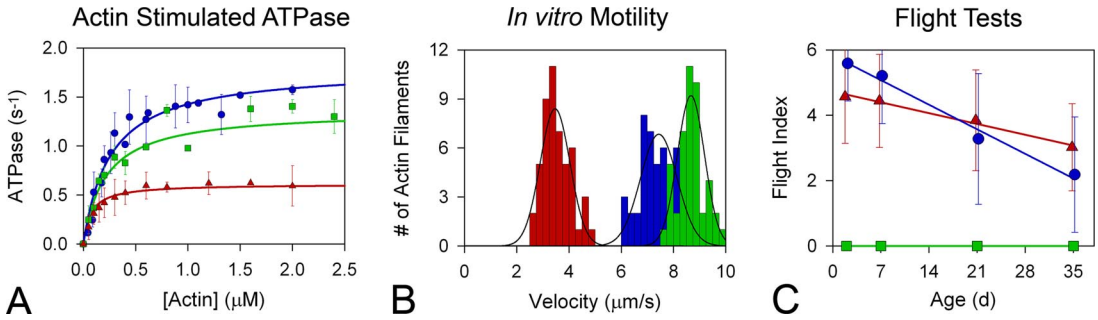

Figure 2. Effects of myosin transducer mutations on molecular and skeletal muscle function. (A) Steady-state rates of actin-activated myosin ATPase for IFI (●), *D45* (▲) and *Mhc*^{5} (■) myosin molecules. ATPase results are represented with data fitting lines. V_{max} values obtained in actin-stimulated Mg^{2+} ATPase assays by using *D45* myosin are reduced to nearly a third of the values obtained for the IFI, whereas V_{max} values for the *Mhc*^{5} isoform are slightly reduced compared with that of the IFI. K_m values do not differ (see Table 1). (B) Histograms comparing the rates of in vitro actin sliding. Actin sliding velocities for IFI are shown in blue, *D45* in red, and *Mhc*^{5} in green. Velocity values (see Table 1) were calculated from roughly 50 continuously moving actin filaments compiled from at least three different assays from at least three independent preparations of each myosin isoform. *D45* myosin translocates F-actin at a velocity about half that of the IFI. However, *Mhc*^{5} myosin drives F-actin movement at a velocity 15% faster than IFI. The average sliding velocities obtained for the three myosin isoforms differ significantly ($p < 0.001$). See Table 1 for details. (C) Effect of depressed or enhanced myosin motor function on flight ability. FIs were calculated for yw (●), *D45* (▲), and *Mhc*^{5} (■) at 2 d, 1 wk, 3 wk, and 5 wk of age. Linear regression analysis reveals both *yw* and *D45* exhibited statistically significant ($p < 0.05$) age-dependent decreases in flight ability. ANCOVA analysis showed significant ($p < 0.05$) heterogeneity in rates (slopes) of flight ability loss over time with the rate of FI decrease being significantly higher in *yw* flies compared with *D45*.

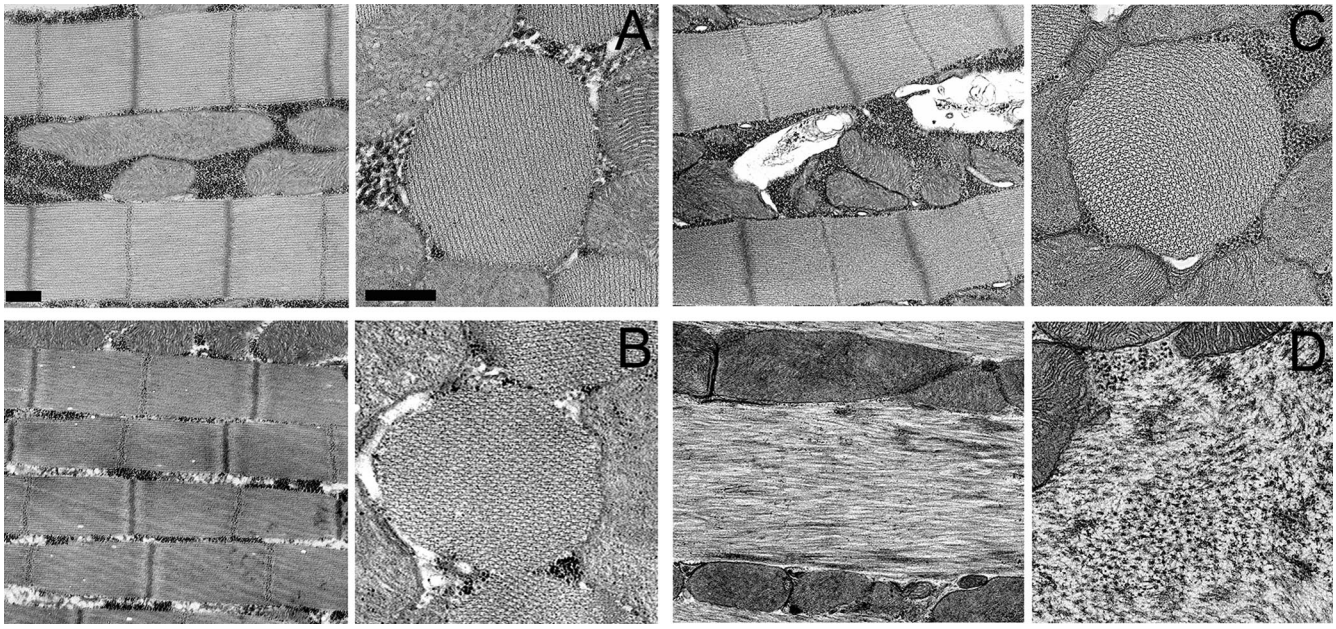

Figure 3. Ultrastructure of IFM myofibrils from flies expressing IFI and mutant myosin isoforms. (A) Longitudinal section (left) of wild-type IFM myofibrils at 2 d after eclosion displays easily discernible sarcomeric M-lines and I-, A-, and Z-band structures. Cross section (right) of *yw* myofibrils shows the characteristic double hexagonal array of thin and thick filaments. Bars, 500 nm. (B) Myofibrils from a fly expressing the hypoactive *D45* isoform at 2 d after eclosion seem very similar to those from wild-type IFM in both longitudinal and cross sections. The formation and stability of myofibrils seems normal, with no visible disorganization. (C) Mhc^5 late pupa possesses myofibrils that seem to have assembled normally into well-organized structures. (D) IFM myofibrils from an adult expressing the hyperactive Mhc^5 isoform at 2 d after eclosion. Severe disruption and disorganization of sarcomeric material is observed. Myofibrillar destruction may be due to excessive actomyosin interactions initiated upon wing movement.

seemed highly organized with easily discernible Z-lines, I-bands, A-bands, H-zones, and M-lines. In cross section, *yw* and *D45* myofibrils displayed the normal, crystalline-like double hexagonal array of myofilament packing. Myofibrils containing the Mhc^5 isoform seem to have assembled normally, as shown by longitudinal and cross sections through late pupae (Figure 3C). By 2 d after eclosion, however, adult Mhc^5 IFM displayed a dramatic disarray of contractile filaments with a loss of sarcomeric structure and integrity of Z-lines, I-bands, A-bands, H-zones, and M-lines (Figure 3D). This is reminiscent of the IFM phenotype arising from unregulated cross-bridge cycling and excessive force production (Beall and Fyrberg, 1991).

Morphological and Functional Effects of Mutant Myosin Activity on Cardiac Muscle

To investigate the effects of depressed or enhanced myosin motor function on cardiac muscle, we surgically exposed, imaged, and tracked beating heart wall movements of semi-intact flies by using direct immersion differential interference contrast optics in conjunction with a high speed digital video camera (see Supplemental Movies 1–3). Visual inspection of the ventral aspect of the heart tubes at 10× magnification revealed obvious differences in mutant cardiac morphology as early as 1 wk after eclosion. Hearts expressing hypoactive *D45* myosin seemed considerably dilated compared with wild-type heart tubes (Figure 4A). The *D45* heart walls also qualitatively displayed compromised shortening abilities and thus perturbed systolic function. Hyperactive Mhc^5 myosin expression induced a narrowing of the heart tubes with obvious restricted regions. These restricted segments seemed unable to adequately relax, and they severely perturbed diastolic function. The restricted region was initially confined to abdominal segment three in several Mhc^5 hearts from 1- to 2-wk-old flies. Subsequently, there seemed to be a lateral spread of restriction gradually affecting abdominal segments 2 and 4 of the heart tubes. The overall incidence of the phenotype increased with advancing age such that by 5 wk nearly all hearts showed some sign of restriction and impaired diastolic function.

High-speed videos of contracting heart tubes were used to generate M-mode traces at 3 wk of age (Figure 4B), the age where AIs become increasingly divergent among fly lines (see below; Ocorr *et al.*, 2007). These traces qualitatively display the dynamics of cardiac contractions. M-modes from semi-intact 3-wk-old *yw* and Mhc^5 heart preparations show fairly regular contractions. However, the rhythmic beating pattern progressively worsened with age. By 5 wk, both lines exhibited nonrhythmical heart contractile patterns, which included asystoles and fibrillations, reflected by increased AI (see below). In contrast to *yw* and Mhc^5 flies, M-mode records from 3-wk *D45* mutant hearts exhibited abundantly more nonrhythmical beating patterns (Figure 4B). Consistent with a substantial AI increase over time (see below) the incidence of arrhythmias became more prevalent by 4 and 5 wk of age in the *D45* mutants compared with the other lines.

To confirm the qualitative differences seen among the genotypes, we quantitatively compared the senescent-dependent changes in a number of cardiac parameters from wild-type and mutant hearts. Heart diameters at 1 through 5 wk of age were measured from individual video frames at peak diastolic and systolic time points. All three genotypes exhibited significant decreases in both diastolic and systolic dimensions with age, reflecting a narrowing of the cardiac chamber (Figure 5A). At every age point studied, however,

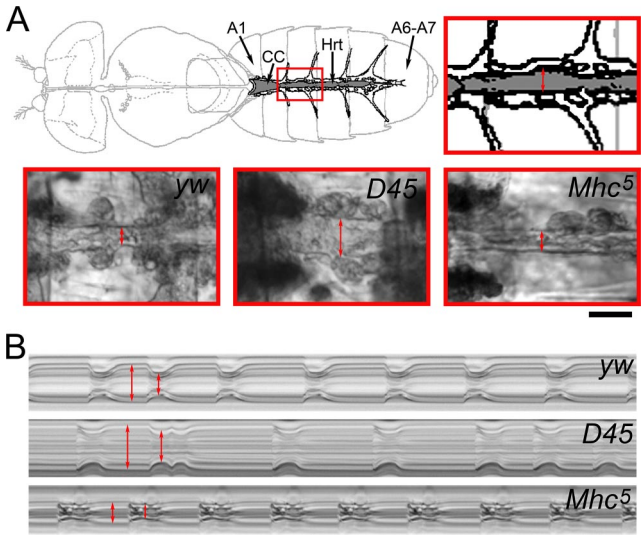

Figure 4. Wild-type and mutant heart morphology and function. (A) Top, schematic of the *D. melanogaster* heart tube, located along the dorsal midline of the abdomen, and the supportive alary muscles (modified from Miller, 1950). Hrt, *Drosophila* heart tube; A1, abdominal segment 1; A6–A7, abdominal segments 6 and 7; and CC, conical chamber of the heart tube. Abdominal segment three of the heart tube is outlined in red and enlarged to demonstrate the region analyzed via motion detection software. The double-headed arrow delineates the heart walls. Bottom, images of A3 heart segments of *yw*, *D45*, and Mhc^5 hearts captured during systole. Note similar systolic wall distances (double-headed red arrows) of *yw* and Mhc^5 heart tubes compared with the dilated systolic distance of the *D45* tube. Bar, 50 μm. (B) M-mode traces showing cardiac cycle dynamics of 3-wk-old *yw*, *D45*, and Mhc^5 hearts. These reveal the locations and movements of the heart walls over a 5-s time period. Note fairly regular heart periods and rhythmicities of *yw* and Mhc^5 heart tubes. However, the extent of diastolic relaxation and fractional shortening seems severely abnormal in Mhc^5 compared with *yw* hearts. Mhc^5 systolic intervals are prolonged. *D45* hearts show dilated systolic and diastolic distances between heart walls and reduced fractional shortening. Additionally, the *D45* cardiac contraction cycles show an arrhythmic pattern with alternating extended and decreased heart periods.

D45 heart walls showed increased mean diastolic and systolic distances, whereas Mhc^5 displayed only decreased diastolic diameters relative to wild type. Both wild-type and Mhc^5 hearts showed an age-related decrease in fractional shortening, with Mhc^5 hearts displaying severely compromised ejection abilities throughout life compared with control hearts (Figure 5B). Fractional shortening for *D45* hearts was substantially perturbed at younger ages, relative to that of wild-type hearts; yet, the tubes showed no overall age-related decrease in contractility.

We characterized the inherent myogenic contractile dynamics and properties of semi-intact hearts by measuring several cardiac parameters from movies of wild-type and mutant flies from 1 through 5 wk of age. The mean HPs of both *yw* and Mhc^5 flies increased moderately and significantly with age (Figure 5C). In contrast, flies expressing hypoactive *D45* myosin exhibited a dramatic and highly significant age-dependent increase in HP compared with age-matched controls. Separating HPs into individual DIs and SIs revealed distinct differences between *yw* and Mhc^5 age-dependent cardiac dynamics (Figure 5, D and E). Over the 5-wk time period, no significant differences were found between DI increases in wild-type and Mhc^5 hearts. Hearts from both lines showed similar significant rate increases in SI; however, at all five age points the Mhc^5 mean SI was significantly longer than that for *yw*. Thus, the increase in Mhc^5 SI substantially contributed to the prolonged HP seen with advancing age in these mutants. *D45* hearts showed significant increases in both DI and SI, a hallmark of failing myocardium. The highly prolonged DI for older *D45* hearts was predominately responsible for the progressive and dramatic increase in HP of these mutants.

To explore senescent-dependent increases in heart rhythm irregularities, we compared the AIs of the three lines (Figure 5F). In both wild-type and Mhc^5 flies, the AI increased progressively, with no significant differences in rates or overall amounts. The AI for *D45* mutant hearts was roughly the same as for control flies at 1 wk of age, and then it increased considerably and significantly compared with control flies, throughout life. Thus, the incidence of arrhythmic cardiac beating patterns increased with age in both wild type and in the mutants, but the extent of increase was much greater in *D45* flies.

As discussed below, diminished molecular motor function of *D45* myosin in our model system seemed to induce a cardiac phenotype similar to that found in humans with dilated cardiomyopathy (Fatkin and Graham, 2002; Ahmad *et al*., 2005; Chang and Potter, 2005). Enhanced molecular properties of Mhc^5 myosin, however, generated pathological hallmarks seemingly analogous to those found in patients suffering from the clinically rare restrictive cardiomyopathy (Kushwaha *et al*., 1997; Fatkin and Graham, 2002; Ahmad *et al*., 2005).

DISCUSSION

Here, we have demonstrated that the myosin transducer is intimately involved with determining the motor's biochemical and mechanical properties and hence the structure and performance of striated muscles. The *Drosophila* transducer is encoded by constitutively expressed exons so that mutations likely alter the kinetic and mechanical properties in a similar manner in all fly striated muscle motors. Therefore, *Drosophila* is a valuable model system to explore dysfunction of multiple muscles resulting from enhanced or depressed motor activity. This is particularly beneficial because similar alterations in myosin performance are associated with the development and age-related progression of numerous skeletal and cardiac myopathies found in higher organisms (Sellers, 1999; Redowicz, 2002; Oldfors *et al*., 2004; Chang and Potter, 2005; Laing and Nowak, 2005; Tardiff, 2005; Oldfors, 2007).

The Mhc^5 mutation maps close to the junction between the HF helix and hypervariable loop 1, a critical element of the transducer. Biochemical and structural studies of wild-type and engineered myosins have shown loop 1 to be involved in kinetic tuning of the motor by influencing a wide range of myosin activities (Kurzawa-Goertz *et al*., 1998; Sweeney *et al*., 1998; Clark *et al*., 2005). The size and flexibility of loop 1 can affect the rate of ATP hydrolysis, product release, actin filament translocation, access to the nucleotide pocket and nucleotide binding affinity (Sweeney *et al*., 1998). Larger and more flexible loops were shown to enhance product release (Sweeney *et al*., 1998). The Mhc^5 transducer mutation may straighten the C-terminal segment of the HF helix and increase the length and/or flexibility of loop 1, thereby enhancing the molecular motor's properties.

The *D45* transducer mutation is located at the β-bulge/β-strand 7 junction and leads to depressed motor activity. Structural studies showed the transducer's loops and linkers interact with each other and undergo coupled distortions to

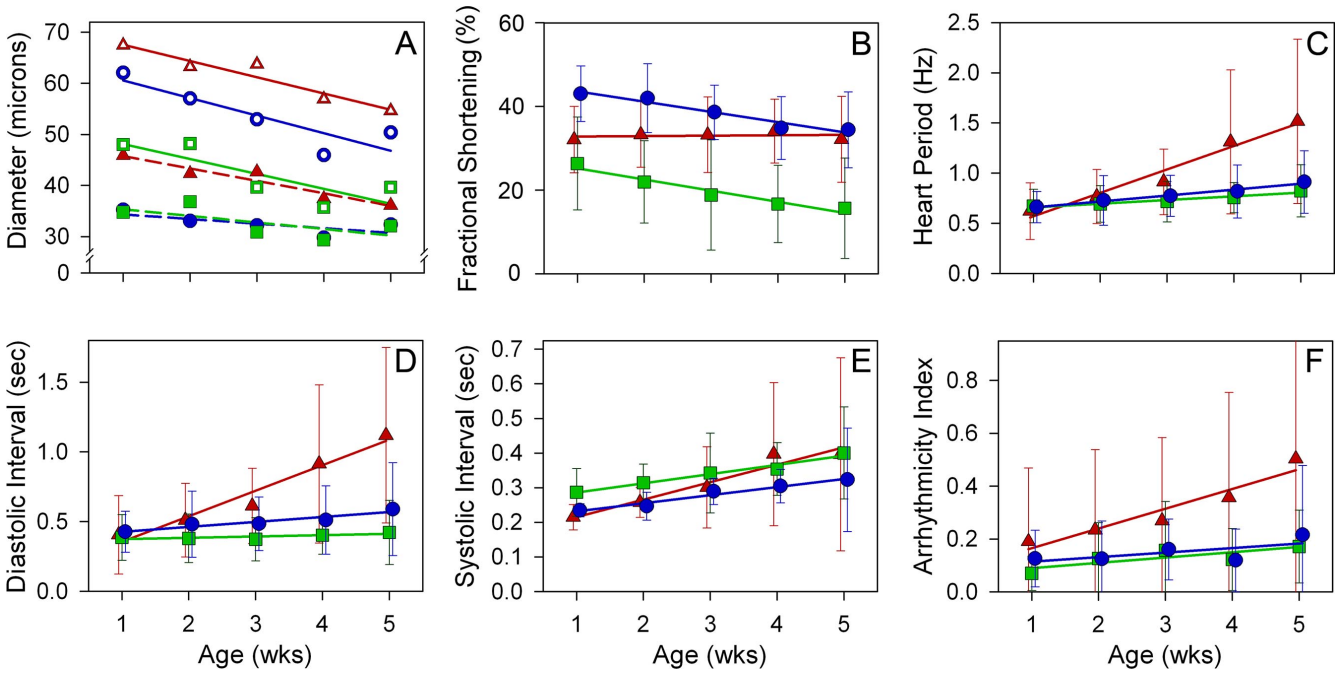

Figure 5. Analysis of age-dependent changes in physiological parameters of *yw* (●), *D45* (▲), and *Mhc*^{5} (■) hearts. Measurements were made on 28–33 hearts from each *Drosophila* line at 1, 2, 3, 4, and 5 wk of age. The means were jittered to facilitate SD comparison. Mean values for each genotype were fit with a linear function and color coded so changes with age could be easily compared. Values of $p < 0.05$ were considered significant. (A) The mean diastolic and systolic diameters are denoted by open or closed symbols, respectively. Solid lines denote diastolic diameter changes, whereas dotted lines reflect systolic diameter changes, with age. All genotypes showed the same significant rate of mean diastolic diameter decrease with age. However, *D45* diastolic heart diameters were significantly greater, whereas *Mhc*^{5} values were significantly less than for *yw* over all age points. There were no significant differences in mean systolic dimensions between *yw* and *Mhc*^{5} hearts over time. Both lines showed identical significant age-dependent decreases in systolic diameter. The mean systolic diameter of *D45* hearts was significantly greater than that of *yw* hearts and the rate of diameter decrease with age was higher for the mutant. (B) Percentage of fractional shortening decreased significantly with age and at the same rate for both *yw* and *Mhc*^{5} hearts; the extent of overall shortening was significantly less for *Mhc*^{5} hearts. *D45* hearts showed no significant age-dependent change in fractional shortening. (C) Both *yw* and *Mhc*^{5} flies displayed the same significant increase in HP with age. The rate and extent of increase for *D45* flies were significantly higher than for control flies. (D) *yw* and *Mhc*^{5} hearts had significant increases in DI, which with age, increased overall at the same rate and to the same extent. *D45* hearts exhibited a significantly greater age-dependent increase in DI compared with wild type. (E) *yw* and *Mhc*^{5} hearts showed identical, significant age-related rate increases in SI. The linear function for *Mhc*^{5} SI, however, was significantly elevated with respect to *yw*. A week-by-week ANOVA confirmed significantly longer mean SI for *Mhc*^{5} hearts at every age point, relative to *yw*. SI for *D45* hearts also showed an age-associated increase that took place at a significantly higher rate than that for *yw* hearts. (F) AI for *yw* and *Mhc*^{5} hearts increased significantly over time, at the same rate, and to the same extent. The AI for *D45* hearts also increased significantly with age, but it increased by a significantly larger amount over time compared with control hearts.

accommodate the distortion of the central β-sheet that occurs during the ATPase cycle (Coureux *et al*., 2003, 2004). The *D45* mutation may disrupt vital interactions between distinct transducer elements, disturbing the coordinated distortion of the mutant transducer and the resulting sequential release of products from the nucleotide-binding pocket during force generation (Coureux *et al*., 2004).

The altered motor activity of the *Drosophila* mutants affected skeletal muscle locomotory function. At young ages, perturbed motor function decreased or eliminated flight ability in *D45* or *Mhc*^{5} flies, respectively. Both wild-type and *D45* flies displayed a characteristic age-dependent reduction in flight ability. Such reductions correlate with declines in glycogen levels and in mitochondrial efficiency and with low myofibrillar protein turnover rates and increased levels of oxidative damage to proteins and lipids (Baker, 1976; Magwere *et al*., 2006). Protein oxidation, which leads to inactivation of certain enzyme systems and to structural protein damage, is considered critical for the aging process (Stadtman, 1992; Levine and Stadtman, 2001; Magwere *et al*., 2006). Thus, extreme physical activity, like flight, poses an inherent, deleterious threat to muscle function. Expression of *D45* myosin with depressed motor function may diminish IFM contraction rates and flight capacity, and also metabolic demands, metabolic by-product accumulation, and associated oxidative damage to proteins and lipids of muscle cells. Therefore, the functional decline normally associated with IFM may be decelerated by hypoactive myosin, and in general, motors with diminished molecular properties could provide age-dependent protection in demanding muscles that normally operate at very high contraction rates.

Electron microscopic examination of *D45* IFM revealed that depressed myosin activity does not perturb IFM sarcomeric structure. In contrast, although *Mhc*^{5} IFM expressing myosin with enhanced molecular function developed normally in the pupa, sarcomeric structure was suddenly destroyed in an apparent use-initiated manner in newly eclosed adults. The ultrastructural phenotype of *Mhc*^{5} IFM seems similar to that found in the hypercontracted IFM of *hdp*^{2} troponin mutants; both phenotypes have been suggested to result from altered actomyosin interactions (Beall and Fyrberg, 1991; Nongthomba *et al*., 2003; Montana and Littleton, 2004). *hdp*^{2} IFM thin filaments exhibit perturbed contractile regulation by troponin-tropomyosin such that

myosin binding sites remain unblocked in both the absence and presence of activating Ca^{2+} (Cammarato *et al.*, 2004). Thus, cross-bridge cycling and force generation would proceed uninhibited and may initiate IFM hypercontraction. Similarly, enhanced kinetic and mechanical properties of Mhc^5 myosin may induce excessive cross-bridge cycling and promote cooperative and constitutive activation of thin filaments and force generation. Consequently the contractile system would remain fully activated and, as with hdp^2 IFM, which are incapable of relaxing, the fibers could quickly destroy themselves and flight ability would be lost.

Expression of *D45* myosin with diminished biomechanical properties produced a *Drosophila* cardiac phenotype displaying structural and functional characteristics remarkably similar to those found in humans with, and in vertebrate models of, dilated cardiomyopathy (DCM) (Fatkin and Graham, 2002; Ahmad *et al.*, 2005; Chang and Potter, 2005; Schmitt *et al.*, 2006; Debold *et al.*, 2007). DCM is a myocardial disorder characterized by left and/or right ventricular dilation and distended chambers (Fatkin and Graham, 2002; Ahmad *et al.*, 2005; Chang and Potter, 2005). Cardiac contractility is depressed, resulting in systolic dysfunction, reduced fractional shortening, and diminished ejection fractions. Affected individuals demonstrate progressive symptoms and gradually develop heart failure, often associated with life-threatening cardiac arrhythmias.

At least 30% of DCM cases are genetic in origin, with more than 15 autosomal dominant missense mutations localized to the β-cardiac *Mhc* gene (Kamisago *et al.*, 2000; Ahmad *et al.*, 2005; Chang and Potter, 2005). Disrupted contractile performance of the diseased myocardium may result from alterations in the mutant myosin's ability to generate force and motion (Schmitt *et al.*, 2006; Debold *et al.*, 2007). Mouse models engineered with DCM-causing β-cardiac MHC mutations reproduced morphological and functional characteristics consistent with the human phenotype (Schmitt *et al.*, 2006). At the molecular level, the mutations depressed ATPase activities, in vitro actin filament sliding velocities, and/or maximal force generating capacity of myosin motors (Schmitt *et al.*, 2006; Debold *et al.*, 2007). Depressing one or more of these molecular indices of myosin function was considered sufficient to trigger the cascade of events that lead to DCM (Debold *et al.*, 2007). Our analysis of *D45 Drosophila* mutants corroborates this hypothesis. *D45* myosin showed substantial decreases in basal and actin-stimulated ATPase rates, and a significant drop in actin sliding velocity. The hearts in turn developed a dilated morphology and functional deficits that worsened with age, consistent with DCM. Thus, the pathological response to depressed motor function seems to be surprisingly similar to that found in higher organisms.

Additional studies have demonstrated a dilatory cardiac response in *Drosophila* resulting from an N-terminal mutation in the TnI inhibitory troponin subunit of the regulatory complex (Wolf *et al.*, 2006). This *Drosophila* cardiac response is consistent with an N-terminal DCM-causing mutation in human cardiac TnI (cTnI) (Murphy *et al.*, 2004; Wolf *et al.*, 2006). *Drosophila* may, therefore, serve as a powerful model for investigating an apparently conserved age-associated cascade of events and cardiac remodeling that occur in response to altered myosin or troponin function that result in specific cardiomyopathies.

In vertebrates, some hypertrophic cardiomyopathy myosin mutations have been shown to increase motor ATPase activities, actin sliding velocities, and/or maximal force generating capacities, suggesting the molecular defects result in a gain of myosin function (Fatkin and Graham, 2002; Ahmad *et al.*, 2005; Debold *et al.*, 2007). Thus, augmented biophysical properties of individual myosin motors potentially initiate hypertrophic cardiac remodeling. *Drosophila* heart tubes, however, expressing Mhc^5 myosin with enhanced biomechanical properties exhibited a cardiac phenotype displaying structural and functional characteristics remarkably similar to those in human restrictive cardiomyopathy (RCM). RCM is a rare myocardial disorder characterized by cardiac remodeling, decreased myocardial wall elasticity, impaired diastolic ventricular filling, and elevated systemic and pulmonary venous pressures (Kushwaha *et al.*, 1997; Fatkin and Graham, 2002; Ahmad *et al.*, 2005). Cardiac rhythmicity, systolic function, and myocardial wall thickness seem unaffected; however, stroke volume and cardiac output are reduced as a result of diastolic dysfunction and restricted filling. The prognosis for RCM patients is poor in that the majority of them experience progressive deterioration of cardiac function and heart failure with a high incidence of premature mortality.

Six missense cTnI mutations were identified in patients with autosomal dominant RCM (Mogensen *et al.*, 2003). Reconstituted troponin complexes with RCM cTnI were unable to properly inhibit actomyosin ATPase (Gomes *et al.*, 2005). Replacing endogenous cTnIs with the RCM cTnIs, in skinned cardiac fibers revealed elevated levels of basal force production (Gomes *et al.*, 2005; Yumoto *et al.*, 2005). Furthermore, relative to wild-type, the RCM cTnI mutations significantly increased the Ca^{2+} sensitivity of force development in skinned cardiac fibers. The impaired myocardial relaxation seen in RCM patients was proposed to result from an inability of the mutant troponin complex to properly inhibit basal ATPase and force development at low Ca^{2+} concentrations (Gomes *et al.*, 2005). A recent study on membrane intact cardiomyocytes expressing an RCM cTnI mutation indeed resulted in thin filament disinhibition and a Ca^{2+}-independent precontracted basal state (Davis *et al.*, 2007).

Our Mhc^5 results suggest that increased motor function could also be involved in RCM development. Enhanced kinetic and mechanical activity of this myosin, consistent with inducing IFM hypercontraction, probably promotes excessive cross-bridge cycling in the mutant hearts. Cross-bridge binding physically impedes troponin-tropomyosin regulatory strand movement back to its blocking position on thin filaments and it increases the affinity of troponin for Ca^{2+}, especially in cardiac muscle (Tobacman, 1996; Moss *et al.*, 2004; Hinken and Solaro, 2007). Enhanced myosin cycling may therefore cooperatively promote its own activity by disproportionately increasing the number of available binding sites on actin and by enhancing the Ca^{2+} sensitivity of the system. Consequently, this could promote the onset of systole and delay relaxation and diastole, prolonging the systolic interval. Mhc^5 hearts displayed significantly prolonged systolic intervals, similar to those in children with heart failure secondary to RCM (Friedberg and Silverman, 2006). Thus, excessive actin–myosin interactions caused by enhanced motor activity, heightened Ca^{2+} sensitivity, and/or thin filament disinhibition, possibly initiating high levels of basal tension and extended systolic intervals, may be major determinants of the diastolic dysfunction seen in Mhc^5 hearts, and they are likely key components in the pathogenesis of RCM. Myosin mutations have never been associated with the development of RCM. However, because impaired myosin or TnI function induces an apparently evolutionarily conserved dilatory response in the *Drosophila* model system, myosin mutations that enhance motor properties should also be considered legitimate candidates in the etiology of the clinically rare RCM.

ACKNOWLEDGMENTS

We thank Douglas Deutschman (San Diego State University) and Douglas M. Swank (Rensselaer Polytechnic Institute) for help with statistical analysis, Chi Lee (San Diego State University) for technical assistance, and Mary C. Reedy (Duke University) for helpful comments and discussions regarding manuscript preparation. This work was supported by a postdoctoral fellowship from the Western States Affiliate of the American Heart Association and National Institutes of Health (NIH) research supplement AR-43396-S1 (to A.C.), NIH grant R01 AR-43396 and NIH grant R01 GM-32443 (to S.I.B.), and NIH grants R01 HL-54732 and P01 AG-15434 (to R.B.).

REFERENCES

Ahmad, F., Seidman, J. G., and Seidman, C. E. (2005). The genetic basis for cardiac remodeling. Annu. Rev. Genomics Hum. Genet. *6*, 185–216.

Baker, G. T., 3rd. (1976). Insect flight muscle: maturation and senescence. Gerontology *22*, 334–361.

Beall, C. J., and Fyrberg, E. (1991). Muscle abnormalities in *Drosophila melanogaster heldup* mutants are caused by missing or aberrant troponin-I isoforms. J. Cell Biol. *114*, 941–951.

Bernstein, S. I., Mogami, K., Donady, J. J., and Emerson, C. P., Jr. (1983). *Drosophila* muscle myosin heavy chain encoded by a single gene in a cluster of muscle mutations. Nature *302*, 393–397.

Brown, J. H., and Cohen, C. (2005). Regulation of muscle contraction by tropomyosin and troponin: how structure illuminates function. Adv. Protein Chem. *71*, 121–159.

Cammarato, A., Hatch, V., Saide, J., Craig, R., Sparrow, J. C., Tobacman, L. S., and Lehman, W. (2004). *Drosophila* muscle regulation characterized by electron microscopy and three-dimensional reconstruction of thin filament mutants. Biophys. J. *86*, 1618–1624.

Chang, A. N., and Potter, J. D. (2005). Sarcomeric protein mutations in dilated cardiomyopathy. Heart Fail. Rev. *10*, 225–235.

Clark, R., Ansari, M. A., Dash, S., Geeves, M. A., and Coluccio, L. M. (2005). Loop 1 of transducer region in mammalian class I myosin, Myo1b, modulates actin affinity, ATPase activity, and nucleotide access. J. Biol. Chem. *280*, 30935–30942.

Coureux, P. D., Sweeney, H. L., and Houdusse, A. (2004). Three myosin V structures delineate essential features of chemo-mechanical transduction. EMBO J. *23*, 4527–4537.

Coureux, P. D., Wells, A. L., Menetrey, J., Yengo, C. M., Morris, C. A., Sweeney, H. L., and Houdusse, A. (2003). A structural state of the myosin V motor without bound nucleotide. Nature *425*, 419–423.

Cripps, R. M., Becker, K. D., Mardahl, M., Kronert, W. A., Hodges, D., and Bernstein, S. I. (1994). Transformation of *Drosophila melanogaster* with the wild-type myosin heavy-chain gene: rescue of mutant phenotypes and analysis of defects caused by overexpression. J. Cell Biol. *126*, 689–699.

Davis, J., Wen, H., Edwards, T., and Metzger, J. M. (2007). Thin filament disinhibition by restrictive cardiomyopathy mutant R193H troponin I induces Ca^{2+}-independent mechanical tone and acute myocyte remodeling. Circ. Res. *100*, 1494–1502.

Debold, E. P., Schmitt, J. P., Patlak, J. B., Beck, S. E., Moore, J. R., Seidman, J. G., Seidman, C., and Warshaw, D. M. (2007). Hypertrophic and dilated cardiomyopathy mutations differentially affect the molecular force generation of mouse alpha-cardiac myosin in the laser trap assay. Am. J. Physiol. *293*, H284–H291.

Drummond, D. R., Hennessey, E. S., and Sparrow, J. C. (1991). Characterisation of missense mutations in the *Act88F* gene of *Drosophila melanogaster*. Mol. Gen. Genet. *226*, 70–80.

Fatkin, D., and Graham, R. M. (2002). Molecular mechanisms of inherited cardiomyopathies. Physiol. Rev. *82*, 945–980.

Finch, C. E., and Ruvkun, G. (2001). The genetics of aging. Annu. Rev. Genomics Hum. Genet. *2*, 435–462.

Friedberg, M. K., and Silverman, N. H. (2006). The systolic to diastolic duration ratio in children with heart failure secondary to restrictive cardiomyopathy. J. Am. Soc. Echocardiogr. *19*, 1326–1331.

Geeves, M. A., Fedorov, R., and Manstein, D. J. (2005). Molecular mechanism of actomyosin-based motility. Cell Mol. Life Sci. *62*, 1462–1477.

Geeves, M. A., and Holmes, K. C. (1999). Structural mechanism of muscle contraction. Annu. Rev. Biochem. *68*, 687–728.

Geeves, M. A., and Holmes, K. C. (2005). The molecular mechanism of muscle contraction. Adv. Protein Chem. *71*, 161–193.

George, E. L., Ober, M. B., and Emerson, C. P., Jr. (1989). Functional domains of the *Drosophila melanogaster* muscle myosin heavy-chain gene are encoded by alternatively spliced exons. Mol. Cell. Biol. *9*, 2957–2974.

Gomes, A. V., Liang, J., and Potter, J. D. (2005). Mutations in human cardiac troponin I that are associated with restrictive cardiomyopathy affect basal ATPase activity and the calcium sensitivity of force development. J. Biol. Chem. *280*, 30909–30915.

Gordon, A. M., Homsher, E., and Regnier, M. (2000). Regulation of contraction in striated muscle. Physiol. Rev. *80*, 853–924.

Hinken, A. C., and Solaro, R. J. (2007). A dominant role of cardiac molecular motors in the intrinsic regulation of ventricular ejection and relaxation. Physiology *22*, 73–80.

Kamisago, M. *et al*. (2000). Mutations in sarcomere protein genes as a cause of dilated cardiomyopathy. N. Engl. J. Med. *343*, 1688–1696.

Kronert, W. A., Acebes, A., Ferrus, A., and Bernstein, S. I. (1999). Specific myosin heavy chain mutations suppress troponin I defects in *Drosophila* muscles. J. Cell Biol. *144*, 989–1000.

Kurzawa-Goertz, S. E., Perreault-Micale, C. L., Trybus, K. M., Szent-Gyorgyi, A. G., and Geeves, M. A. (1998). Loop I can modulate ADP affinity, ATPase activity, and motility of different scallop myosins. Transient kinetic analysis of S1 isoforms. Biochemistry *37*, 7517–7525.

Kushwaha, S. S., Fallon, J. T., and Fuster, V. (1997). Restrictive cardiomyopathy. N. Engl. J. Med. *336*, 267–276.

Laing, N. G., and Nowak, K. J. (2005). When contractile proteins go bad: the sarcomere and skeletal muscle disease. Bioessays *27*, 809–822.

Levine, R. L., and Stadtman, E. R. (2001). Oxidative modification of proteins during aging. Exp. Gerontol. *36*, 1495–1502.

Magwere, T., Pamplona, R., Miwa, S., Martinez-Diaz, P., Portero-Otin, M., Brand, M. D., and Partridge, L. (2006). Flight activity, mortality rates, and lipoxidative damage in *Drosophila*. J. Gerontol. A Biol. Sci. Med. Sci. *61*, 136–145.

Margossian, S. S., and Lowey, S. (1982). Structural and contractile proteins. In: Methods in Enzymology, Vol. 85, ed. L. W. Cunningham and D. W. Frederiksen, New York: Academic Press, 55–70.

McKillop, D. F., and Geeves, M. A. (1993). Regulation of the interaction between actin and myosin subfragment *1*, evidence for three states of the thin filament. Biophys. J. *65*, 693–701.

Miller, A. (1950). The internal anatomy and histology of the imago of *Drosophila melanogaster*. In: Biology of *Drosophila*, ed. M. Demerec, New York: Wiley, 420–534.

Mogensen, J., Kubo, T., Duque, M., Uribe, W., Shaw, A., Murphy, R., Gimeno, J. R., Elliott, P., and McKenna, W. J. (2003). Idiopathic restrictive cardiomyopathy is part of the clinical expression of cardiac troponin I mutations. J. Clin. Invest. *111*, 209–216.

Montana, E. S., and Littleton, J. T. (2004). Characterization of a hypercontraction-induced myopathy in *Drosophila* caused by mutations in *Mhc*. J. Cell Biol. *164*, 1045–1054.

Moss, R. L., Razumova, M., and Fitzsimons, D. P. (2004). Myosin crossbridge activation of cardiac thin filaments: implications for myocardial function in health and disease. Circ. Res. *94*, 1290–1300.

Murphy, R. T., Mogensen, J., Shaw, A., Kubo, T., Hughes, S., and McKenna, W. J. (2004). Novel mutation in cardiac troponin I in recessive idiopathic dilated cardiomyopathy. Lancet *363*, 371–372.

Nongthomba, U., Cummins, M., Clark, S., Vigoreaux, J. O., and Sparrow, J. C. (2003). Suppression of muscle hypercontraction by mutations in the myosin heavy chain gene of *Drosophila melanogaster*. Genetics *164*, 209–222.

Ocorr, K., Reeves, N. L., Wessells, R. J., Fink, M., Chen, H. S., Akasaka, T., Yasuda, S., Metzger, J. M., Giles, W., Posakony, J. W., and Bodmer, R. (2007). KCNQ potassium channel mutations cause cardiac arrhythmias in *Drosophila* that mimic the effects of aging. Proc. Natl. Acad. Sci. USA *104*, 3943–3948.

Oldfors, A. (2007). Hereditary myosin myopathies. Neuromuscul. Disord. *17*, 355–367.

Oldfors, A., Tajsharghi, H., Darin, N., and Lindberg, C. (2004). Myopathies associated with myosin heavy chain mutations. Acta Myol. *23*, 90–96.

Pardee, J. D., and Spudich, J. A. (1982). Structural and contractile proteins. In: Methods in Enzymology, Vol. 85, ed. L. W. Cunningham and D. W. Frederiksen, New York: Academic Press, 164–179.

Parkes, T. L., Hilliker, A. J., and Phillips, J. P. (1999). Motorneurons, reactive oxygen, and life span in *Drosophila*. Neurobiol. Aging *20*, 531–535.

Paternostro, G., Vignola, C., Bartsch, D. U., Omens, J. H., McCulloch, A. D., and Reed, J. C. (2001). Age-associated cardiac dysfunction in *Drosophila melanogaster*. Circ. Res. *88*, 1053–1058.

Poole, K. J., Lorenz, M., Evans, G., Rosenbaum, G., Pirani, A., Craig, R., Tobacman, L. S., Lehman, W., and Holmes, K. C. (2006). A comparison of muscle thin filament models obtained from electron microscopy reconstructions and low-angle X-ray fibre diagrams from non-overlap muscle. J. Struct. Biol. *155*, 273–284.

Redowicz, M. J. (2002). Myosins and pathology: genetics and biology. Acta Biochim. Pol. *49*, 789–804.

Root, D. D., and Wang, K. (1994). Calmodulin-sensitive interaction of human nebulin fragments with actin and myosin. Biochemistry *33*, 12581–12591.

Rozek, C. E., and Davidson, N. (1983). *Drosophila* has one myosin heavy-chain gene with three developmentally regulated transcripts. Cell *32*, 23–34.

Schmitt, J. P. *et al*. (2006). Cardiac myosin missense mutations cause dilated cardiomyopathy in mouse models and depress molecular motor function. Proc. Natl. Acad. Sci. USA *103*, 14525–14530.

Sellers, J. R. (1999). Myosins, Oxford; New York: Oxford University Press.

Stadtman, E. R. (1992). Protein oxidation and aging. Science *257*, 1220–1224.

Suggs, J. A., Cammarato, A., Kronert, W. A., Nikkhoy, M., Dambacher, C. M., Megighian, A., and Bernstein, S. I. (2007). Alternative S2 hinge regions of the myosin rod differentially affect muscle function, myofibril dimensions and myosin tail length. J. Mol. Biol. *367*, 1312–1329.

Swank, D. M., Bartoo, M. L., Knowles, A. F., Iliffe, C., Bernstein, S. I., Molloy, J. E., and Sparrow, J. C. (2001). Alternative exon-encoded regions of *Drosophila* myosin heavy chain modulate ATPase rates and actin sliding velocity. J. Biol. Chem. *276*, 15117–15124.

Swank, D. M., Knowles, A. F., Kronert, W. A., Suggs, J. A., Morrill, G. E., Nikkhoy, M., Manipon, G. G., and Bernstein, S. I. (2003). Variable N-terminal regions of muscle myosin heavy chain modulate ATPase rate and actin sliding velocity. J. Biol. Chem. *278*, 17475–17482.

Sweeney, H. L., Rosenfeld, S. S., Brown, F., Faust, L., Smith, J., Xing, J., Stein, L. A., and Sellers, J. R. (1998). Kinetic tuning of myosin via a flexible loop adjacent to the nucleotide binding pocket. J. Biol. Chem. *273*, 6262–6270.

Tardiff, J. C. (2005). Sarcomeric proteins and familial hypertrophic cardiomyopathy: linking mutations in structural proteins to complex cardiovascular phenotypes. Heart Fail. Rev. *10*, 237–248.

Tatar, M., Bartke, A., and Antebi, A. (2003). The endocrine regulation of aging by insulin-like signals. Science *299*, 1346–1351.

Tobacman, L. S. (1996). Thin filament-mediated regulation of cardiac contraction. Annu. Rev. Physiol. *58*, 447–481.

Vibert, P., Craig, R., and Lehman, W. (1997). Steric-model for activation of muscle thin filaments. J. Mol. Biol. *266*, 8–14.

Wessells, R. J., and Bodmer, R. (2007). Age-related cardiac deterioration: insights from *Drosophila*. Front. Biosci. *12*, 39–48.

Wolf, M. J., Amrein, H., Izatt, J. A., Choma, M. A., Reedy, M. C., and Rockman, H. A. (2006). *Drosophila* as a model for the identification of genes causing adult human heart disease. Proc. Natl. Acad. Sci. USA *103*, 1394–1399.

Yumoto, F. *et al*. (2005). Drastic Ca^{2+} sensitization of myofilament associated with a small structural change in troponin I in inherited restrictive cardiomyopathy. Biochem. Biophys. Res. Commun. *338*, 1519–1526.